Eur Biophys J (2000) 28: 621–628

ARTICLE

F. Barone · L. Cellai · C. Giordano
M. Matzeu · F. Mazzei · F. Pedone

γ-Ray footprinting and fluorescence polarization anisotropy of a 30-mer synthetic DNA fragment with one 2′-deoxy-7-hydro-8-oxoguanosine lesion

Received: 14 April 1999 / Revised version: 27 September 1999 / Accepted: 27 September 1999

Abstract The influence of the oxidative lesion 2′-deoxy-7-hydro-8-oxoguanosine (8-oxodG) on some conformational properties of DNA has been studied. Four 30-mer duplexes of the form [5′-GATCCTCTAGAG-TC[G* or G]ACCTGCAGGCATGCA-3′]:[3′-CTAG-GAGATCTCAG[C or A]TGGACGTCCGTACGT-5′], in which G* is the 8-oxodG lesion, were synthesized in order to compare the effect of the GA mismatch and of the damaged G*C and G*A forms with the normal GC. Spectroscopic measurements performed by means of UV denaturation and circular dichroism experiments do not show gross changes of stability and overall structure in the damaged and mismatched samples. The control DNA and the samples containing GA mismatch show very similar γ-rays cutting patterns, indicating that the introduction of the GA mismatch does not perturb the phosphate backbone geometry. In the samples containing the 8-oxodG there are some variations of the cleavage pattern near G* which are extended for almost one helical turn. Some differences are observed between G*C and G*A duplexes. In particular, in the G*C sample the reduced accessibility to OH radicals at the G15 site, observed in the control, spreads on the intra-strand adjacent bases and in the G*A sample a shift of the minimum is observed. The hydrodynamic radius R_h derived by fluorescence polarization anisotropy decay exhibits a constant value of 11.4 ± 0.2 Å between 5 and 40 °C, in all the samples. The torsional constant α of each oligomer decreases when the temperature is raised and the α values of the damaged samples are higher than those of the normal ones.

Key words γ-Ray footprinting · Fluorescence polarization anisotropy · DNA damage · Oxidative lesion

F. Barone · M. Matzeu (✉) · F. Mazzei
Laboratorio di Fisica, Istituto Superiore di Sanità,
Viale Regina Elena 299, I-00161 Rome, Italy
e-mail: matzeu@axiss.iss.infn.it

L. Cellai
Istituto di Strutturistica Chimica, CNR, Rome, Italy

C. Giordano
Centro di Studio per la Chimica del Farmaco del CNR,
Università La Sapienza, Rome, Italy

F. Pedone
Istituto Nazionale di Fisica della Materia,
Università La Sapienza, Rome, Italy

Introduction

The study of the mechanisms related to structural and conformational changes of DNA induced by radiation is an important step towards the knowledge of processes promoting mutagenesis and carcinogenesis. Particular interest is devoted to the consequences of oxidative damage on DNA produced by hydroxyl radicals, singlet oxygen, and superoxide which can arise either from cellular metabolism or from radiation and chemical action (von Sonntag 1987; Wang et al. 1998). Apart from ionizing radiation, also UVA light absorbed by endogenous or exogenous photosensitizing molecules causes indirect effects due to energy transfer such as single- and double-strand breaks on the polynucleotide chain and mainly the production of 2′-deoxy-7-hydro-8-oxoguanosine (8-oxodG or G*) (Dizdaroglu 1985; Kasai et al. 1986; Cridland and Saunders 1994; Zhang et al. 1997). The decrease in the stratospheric ozone layer which drives UV flux on the Earth's surface, in addition to wide spread use of photosensitizing substances, have boosted research on the mechanisms and consequences of this type of damage on DNA.

8-oxodG is mutagenic. Many reviews describe the formation, repair, and mutation mechanisms due to the accumulation of this oxidation product (Grollman and Moriya 1993; Grollman et al. 1994; Wang et al. 1998). It can be produced in vivo either by modification of the G base in double-stranded DNA, or by incorporation of 8-oxodGTP during DNA synthesis. In this last case, it is preferentially incorporated in front of A, promoting

TA → GC transversion after the replicative process. A specific repair system (Mut T pathway) directly operates on the 8-oxodGTP pool before incorporation, reducing the probability of this mutation. When 8-oxodG is produced as damage in DNA, another repair system (Mut M) can restore the correct G by means of specific enzymes that recognize the G*C base pair. Otherwise, A instead of C can be synthesized in front of G*, giving rise to a G*A base pair, not recognized by the Mut M repair system. In this case, another repair pathway (Mut Y) can occur by removing A and restoring C (likely in a GA mismatch) in the G*C base pair. Failure of repair in DNA is associated with GC → TA transversion after replication.

Many studies have recently been published, aimed at establishing the structural and/or thermodynamic basis of recognizing such premutagenic lesions. NMR data (Kouchakdjian et al. 1991; Oda et al. 1991; Mc Auley-Hetch et al. 1994) indicate different structural features in 8-oxodG when it binds C or A. Furthermore, it has been shown that the GA base pair conformation may differ from the *anti-anti* one observed in GC and depends on the pH and neighboring intrastrand bases (base step) (Gao and Patel 1988; Brown et al. 1989). As far as the thermodynamic stability is concerned, the observed energetic differences of 8-oxodG samples are not judged to be a sufficient test to elucidate a discriminating mechanism of the repair system (Plum et al. 1995).

In this paper we report a study on duplex 30-mer DNA fragments containing an 8-oxo-modified guanine base by means of various techniques. Our aim was to correlate variations of different properties with the presence of specific damage. DNA fragments contained a native G or modified G* on one strand in a central position (G15) and a corresponding C or A on the complementary strand. We have compared hydrodynamic, spectroscopic, and thermodynamic properties and the duplexes, accessibility to hydroxyl radicals produced by water radiolysis, which are particularly useful for detecting fine structural features of nucleic acid conformation (Franchet-Beuzit et al. 1993; Barone et al. 1994). In order to correlate the single damage effect on DNA internal motion, due to twisting of the double helix, we have measured variations of the torsional constant of the samples by phase fluorometry.

Materials and methods

Materials

The synthesis of the protected phoshoramidite of 2′-deoxy-7-hydro-8-oxoguanosine was performed using standard methods: transient protection (Ti et al. 1982) of 8-(benzyloxy)deoxyguanosine (Lin et al. 1985) with isobutyric anhydride gave the N^2 isobutyryl derivative which, on catalytic hydrogenation, led to N^2-isobutyryl-8-oxo-2′-deoxyguanosine; 4-4′-dimethoxytritylation on 5′-OH in the presence of pyridine and further treatment with 2-cyanoethyl *N*,*N*-diisopropyl chlorophosphoramidite and triethylamine afforded the phosphoramidite required for the synthesis of the oligomers. Automatic synthesis of the oligomers was performed in an ABI 392 apparatus according to the cyanoethyl phosphoramidite chemistry, at the 1 μmol scale. The samples were purified by HPLC on a column of Pure DNA Dynamax-300 A (Rainin), 5 μmol, 21.4 × 50.0 mm, by a gradient of acetonitrile-triethylammonium acetate, 0.1 M, pH 7. The purity was checked by denaturing PAGE and usually the samples to be used contained less than 2% of lower molecular weight fragments.

The following four 30-mer single-strand DNA oligomers were synthesized: 5′-GATCCTCTAGAGTC[G* or G]ACCTGCAGGCATGCA-3′ and 3′-CTAGGA-GATCTCAG[C or A]TGGACGTCCGTACGT-5′ in which G* is the 8-oxodG modified base. Samples were dissolved at a concentration of 1 mg/ml in deionized water. We assume the same extinction coefficient for the oligomers containing G or G* ($\varepsilon = 2.72 \times 10^5\ M^{-1}\ cm^{-1}$) and ε values at 260 nm equal to $2.78 \times 10^5\ M^{-1}\ cm^{-1}$ and $2.85 \times 10^5\ M^{-1}\ cm^{-1}$ for oligomers containing C or A, respectively, in the opposite strands. The ε values were calculated according to Cantor et al. (1970). Annealing of the samples (duplexes are named GC, GA, G*C and G*A) was performed at a 1:1 molar ratio at the desired concentration in the appropriate buffer by heating solutions up to 80 °C and cooling them slowly to 4 °C. Complete annealing of the samples was checked by PAGE in TBE buffer.

Spectroscopic measurements

Circular dichroism (CD) spectra were recorded by means of a Jasco J710 spectropolarimeter between 320 and 200 nm, with a scanning rate of 10 nm/min. The spectral resolution was 0.2 nm and the band width 1 nm. The samples (1.9 μM, in 10 mM Na phosphate, 100 mM NaCl, 0.1 mM EDTA, pH 7) were placed in a cylindrical water-jacketed cell (1 cm path length) and thermostated by means of a Haake H20 bath. Measurements were performed at 10 °C and a nitrogen stream was flushed on the cuvette wall to avoid water condensation.

UV absorption changes at 260 nm were followed by means of a Cary 3 UV/VIS spectrophotometer. Sample thermostation was obtained using a Peltier device and the temperature was raised at a rate of 0.5 °C/min. Absorbance values of the samples were corrected for thermal expansion of the water and normalized at 1 value of optical density at the lower temperature. Thermodynamic analysis was performed according to Breslauer (1994), as already described (Barone et al. 1999).

γ-Ray footprinting

Single-stranded oligomers obtained by HPLC, as already described, were further purified by band excision

from denaturing polyacrylamide gel. The fragments were eluted by an overnight incubation in deionized water at 37 °C. The oligomers were 3′-end-labeled by incubation with [α-P^{32}]ddATP (Amersham) and the terminal transferase enzyme (Boehringer-Mannheim), and then eluted by a Sephadex G-25 column. Annealing of the 3′-end-labeled oligomers with an excess of unlabeled complementary strand was performed in 10 mM sodium phosphate buffer, pH 7. Complete annealing was checked by 15% polyacrylamide gel analysis in non denaturing conditions, 45 mM Tris-Borate, 1 mM EDTA (TBE buffer), pH 8, run at 4 °C for 17 h. Labeled samples, dissolved in 100 μl of buffer, were irradiated, on an ice-water bath, in a GammaCell 220 (AECL), equipped with a ^{60}Co source, at a dose of 180 Gy. The dose rate was about 6.1 Gy/min.

Irradiated samples were electrophoresed at high voltage on 20% denaturing polyacrylamide gels (20 × 40 × 0.04 cm), containing 7 M urea in TBE, as described by Sambrook et al. (1989). The identification of guanine and adenine bases on sequencing gels was performed according to Negri et al. (1991). Gels were run at 27 W, fixed for 10 min in 10% acetic acid, dried at 60 °C, and autoradiographed using Kodak X-OMAT S films and a Kodak X-OMATIC cassette with intensifying screens. In order to achieve the best resolution of the bands, two gels were run for each sample: the first one for 2 h and the second one for 4 h. The densitometric analysis of the autoradiographs was performed by an ULTROSCAN XL (Pharmacia LKB) laser densitometer. As a rule, we discarded the two bands at the 5′-end owing to their poor resolution and the two bands at the 3′-end for their low intensity. In fact, in γ-ray footprinting the dose is delivered in order to produce only one single cut per molecule, so that the amount of very short fragments sharply drops. The reproducibility of independent experiments was within 10%.

The area of each band was evaluated using the public domain NIH Image program (developed at the US National Institute of Health and available on the internet at http://rsb.info.nih.gov/nih-image/). The area values were normalized to the sum of the areas of the measured bands.

Fluorescence dynamic measurements

Lifetime and fluorescence polarization anisotropy measurements were performed by a K2-ISS phase-shift fluorometer instrument (Urbana, Ill., USA) using the 514 nm 0.5 W output of a coherent Innova 90C argon laser. The modulation ratio of the excitation light was always in the range 60–70% and the detection cross-correlation frequency was 80 Hz.

The samples were placed into 1 cm quartz cells and a long-pass filter (550 nm) was set between the sample turret and the photomultiplier to minimize detection of scattered light. The samples, dissolved in 10 mM sodium phosphate, 100 mM NaCl, 0.1 mM EDTA, pH 7 buffer, were thermostated by means of a circulating water bath (Haake K15) within ±1 °C in the range 0–40 °C. Ethidium bromide (EB) was used as fluorophore in a ratio of 1 mole of EB per 200 base pairs, as energy transfer phenomena are absent at this EB/DNA ratio.

Lifetime determination at each temperature was carried out before performing the relative anisotropy measurement in all the samples. For the lifetime measurements, 10 frequencies logarithmically spaced in the 2–40 MHz interval were acquired. The excitation polarizer was set at 35° with respect to vertical polarization of the laser and polystyrene latex was used as reference. The lifetime data were analysed with the ISS fluorometer software running on a PC, considering also the presence in solution of 0.1% of free ethidium with a lifetime equal to 1.7 ns. The lifetime data of the bound dye versus temperature were fitted by a linear regression: $\tau(T) = 24.1 - 0.06T$. This dependence was accounted on the following FPA data analysis.

In the FPA measurements, 20 frequencies were acquired in the 2–40 MHz interval with the excitation polarizer kept fixed at 0° (i.e. vertical) and the emission polarizer automatically rotated at 0° and 90° for each acquisition. The error for phase and modulation was 0.2° and 0.004, respectively, amounting to ≈1% of the signal.

Phase differences and demodulation ratios were fitted with a Vax station in order to obtain the hydrodynamic parameters.

The computation of fluorescence anisotropy decay in the time domain for a realistic DNA model has been given by Allison and Schurr (1979). DNA is assumed to be a series of disks (the base pairs) connected by Hookean springs. This model has been adapted for phase fluorometry by Collini et al. (1995). In general, the fluorescence anisotropy $r(t)$ is given by products (Schurr 1984) of the internal correlation functions $A_n(t)$ related to geometric factors, due to the particular dye intercalating geometry, and of bending $F_n(t)$ and torsional $C_n(t)$ correlation functions:

$$r(t) = \frac{(I_{\parallel} - I_{\perp})}{(I_{\parallel} + 2I_{\perp})} = r_0 \sum_{n=-2}^{2} A_n(t) C_n(t) F_n(t) \qquad (1)$$

where $I_{\parallel}$ and $I_{\perp}$ are the fluorescence intensities measured with the polarizer oriented in parallel and in perpendicular position, respectively, and r_0 is the initial anisotropy value, assumed to be 0.36 due to the isotropic dye wobbling (Madge et al. 1983). The complete mathematical expression of the three correlation functions has been described previously (Barone et al. 1998). Briefly, the internal correlation functions $A_n(t)$ are related to the angle θ formed by the EB dipole and the helix axis, which has been assumed to be 70.5° (Schurr 1984). The torsional correlation functions $C_n(t)$ are related to α, the adjustable torsion constant between base pairs. The DNA torsional rigidity C might be derived by $C = \alpha b$, where b is 3.4 Å. The persistence length was assumed to be 200 nm. The hydrodynamic radius R_h

was derived from the expression reported in the literature for the diffusion coefficients of a cylindrical rigid rod (Tirado and Garcia de la Torre 1980).

Results and discussion

Spectroscopic measurements

CD spectra indicate normal B DNA conformation in all the analysed samples, as shown in Fig. 1. In particular, GC and G*C fragments show very similar spectra, suggesting that guanine oxidation does not alter the Watson-Crick geometry of these samples. It has been shown that normal hydrogen bonds are indeed allowed by the 6–8 diketo form of 8-oxodG predominating under physiological conditions (Culp et al. 1989). Minor differences are observed in the comparison of the GA and G*A samples, too. The observed small variations of the band intensity at 280 and 250 nm might be due to changes in electron distribution related to the presence of the different base opposite to G* or G.

The melting temperature of G*C fragments is only 1.5 °C lower than the control, as shown in Table 1. The change of free energy ΔG (as also ΔH and ΔS) has nevertheless nearly the same value, indicating comparable thermodynamic stability. As observed in Table 1, the lowest stability of the four samples is observed for GA, so that the mismatch GA can be considered more effective than the introduction of oxidative damage from the energetic point of view.

These results show, as expected, that oxidative damage at one guanine site in a 30-mer oligonucleotide does not induce gross changes in its overall conformation or thermodynamic properties. Thus, enzymatic recognition of G* cannot occur via energetic or gross structural alterations, but it can arise from finer local distorsions which can be revealed by means of more specific techniques, such as γ-ray footprinting.

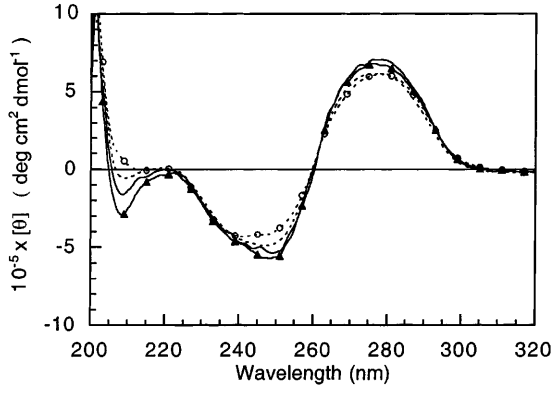

Fig. 1 Molar ellipticity versus wavelength of the DNA fragments. Sample concentration was 1.9 μM in 10 mM sodium phosphate buffer, 0.1 mM EDTA, 100 mM NaCl, pH 7. GC —— : G*C —▲—; GA - - - - - - - ; G*A - - - -○- - - -

Table 1 Thermodynamic parameters calculated by UV melting curves of the control and of 8-oxodG damaged and/or mismatched samples at 1.9 μM concentration in 10 mM sodium phosphate, 0.1 mM EDTA, 100 mM NaCl, pH 7

Sample	T_m (°C)	$-\Delta H$ (kcal mol^{-1})	$-\Delta S$ (kcal mol^{-1} K^{-1})	$-\Delta G_{37}$ (kcal mol^{-1})
GC	73.3 ± 0.5	173 ± 9	0.47 ± 0.02	25.9 ± 1.3
G*C	71.8 ± 0.5	173 ± 9	0.48 ± 0.02	25.4 ± 1.3
GA	67.9 ± 0.5	146 ± 7	0.40 ± 0.02	21.2 ± 1.1
G*A	69.0 ± 0.5	166 ± 8	0.46 ± 0.02	23.6 ± 1.2

γ-Ray footprinting measurements

In γ-ray footprinting, OH radicals interact and cleave the sugar phosphate backbone by extracting a hydrogen atom, preferentially at the C4′ and C5′ positions (Sy et al. 1997) in the minor groove of the double helix. Thus, this technique monitors mainly the minor groove dimensions like width and depth. Figures 2 and 3 show the histograms of the relative cutting frequency versus sequence of the four samples. It can be observed that OH radical attack is variously modulated along the sequence. The G at position 15 resides in a zone where the minor groove is narrow compared to neighboring bases. Furthermore, it is evident that GC and GA exhibit very similar patterns (Fig. 2a, b), suggesting that the presence of C or A as the opposite base does not vary the local groove geometry. It has been reported (Brown et al.

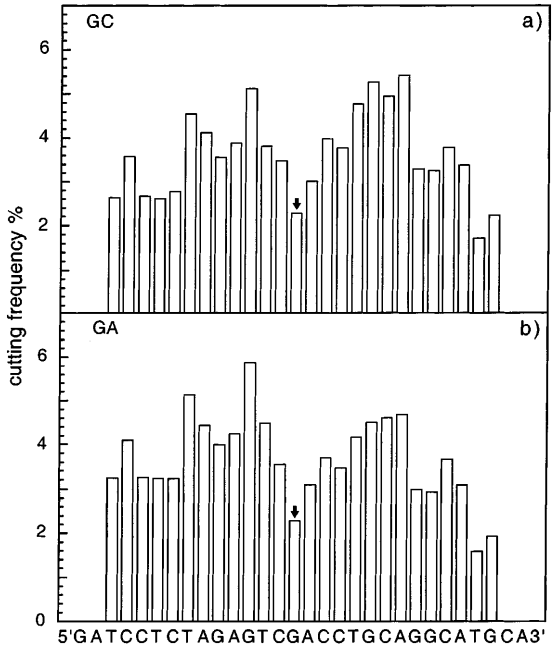

Fig. 2a, b Data analysis of γ-ray footprinting experiments performed in 10 mM sodium phosphate buffer, pH 7. Relative cutting frequency (as deduced by the band area in denaturing polyacrylamide gels) versus sequence in the control and mismatched sample. **a** GC; **b** GA. The *arrow* indicates the mismatch position

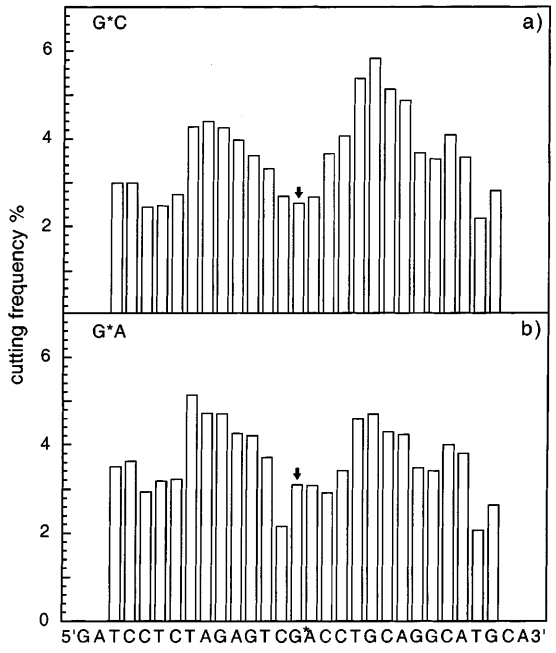

Fig. 3a, b Data analysis of γ-ray footprinting experiments performed in 10 mM sodium phosphate buffer, pH 7. Relative cutting frequency (as deduced by the band area in denaturing polyacrylamide gels) versus sequence in the samples containing 8-oxodG. **a** G*C; **b** G*A. The *arrow* indicates the damage position

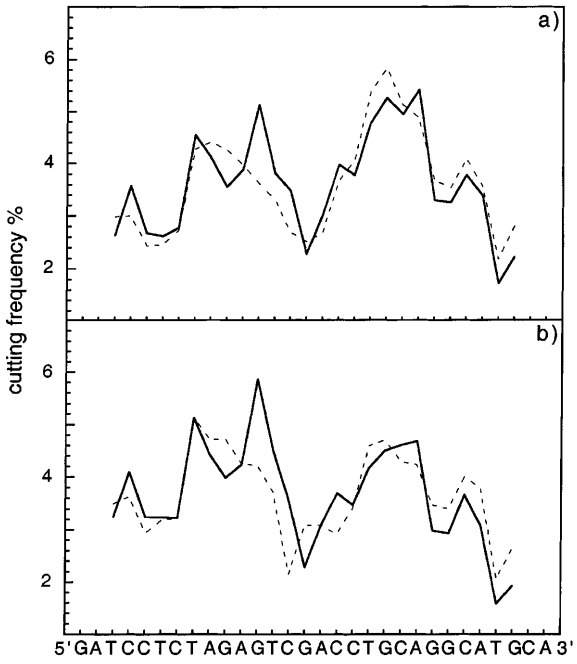

Fig. 4a, b Continuous patterns comparing the relative cutting frequency versus sequence of the samples in γ-ray footprinting experiments performed in 10 mM sodium phosphate, pH 7. **a** GC (——) and G*C (- - - - -) samples; **b** GA (——) and G*A (- - - - -) samples

1986) that some minor structural differences between GC and GA base pairs are confined in the major groove, while the minor groove preserves the same width. Our footprinting data agree with this result. On the contrary, some differences are evident in the cutting pattern of G*C and G*A samples as shown in Fig. 3.

In order to better compare samples containing (or not) the oxidative damage (GC with G*C and GA with G*A), a continuous line connecting the bars has been traced in Fig. 4. A reduced cutting frequency, suggestive of a lower width of the minor groove, is observed at the C14pG15 step, according to molecular modelling results based on NMR and crystallographic data (Bertrand et al. 1998; Packer and Hunter 1998). These studies indicate that CpG and CpA steps in a duplex with overall B conformation can undergo a conformational transition between two forms called BI and BII. These conformations differ mainly for slide and twist between the two adjacent bases and their equilibrium can be influenced by the next neighboring bases. The BII conformation involves a change of the base stacking and a decrease of the minor groove width, so that in our sequence a reduction of accessibility to OH radicals can be expected at four sites: the C14pG15 step and the three CpA steps toward the 3′-end. Narrowing of the minor groove is observed only at the C14pG15 step, owing possibly to its particular neighboring sequence.

In Fig. 4a, b we have compared the GC, G*C and GA, G*A couples respectively in order to determine the effect of the 8-oxodG damage on the normal and mismatched sequences. The major modifications of the cutting frequency occur in a sequence region that spans from T8 to G15 for both modified samples. In particular, both the patterns show a significant reduction of the cutting frequency at the G12 base with a smoothing of the profile in the neighboring region. In a study concerning an 80 base pairs DNA fragment (Sy et al. 1997), it has been shown that the minor groove width, sequence-modulated, approximately spans a range from 2.5 Å to 6.5 Å, corresponding to zero and maximal accessibility for OH radicals, respectively. Assuming the same range for our samples, we can give a gross evaluation of the minor groove reduction at G12 of roughly 1 Å. This result highlights that γ-ray footprinting analysis is comparable in sensitivity with X-rays or NMR techniques and can be employed also for studying longer DNA fragments, in solution.

It has been reported that the GA base pair located in the CpGpA step assumes an *anti-syn* conformation (Brown et al. 1989), while the GC base pair is in an *anti-anti* conformation. The oxidative damage introduction alters the two forms in a different way: (1) in the G*C sample the reduced accessibility at the G15 site, observed in the control, spreads on the intrastrand adjacent bases, (2) in the G*A sample a shift toward the 5′-side of the minimum at the G15 position is observed. These differences could be due to different stacking interactions between G* and the neighboring bases.

Fluorescence measurements

The experimental data of phase and demodulation ratios versus the frequency at different temperatures were fitted

for every sample according to the procedure described in Materials and methods which allows the calculation of the hydration radius (R_h) and torsional constant (α) values. Good χ^2 values around 1 and not exceeding 1.2 were usually obtained in the range of temperature from 0 to 40 °C. The hydration radius of all the samples exhibits a value of 11.4 ± 0.2 Å, constant with the temperature, while some differences are evident for the torsional constant values. In Fig. 5a, b the values of the torsional constant as a function of the temperature are shown and compared for the pairs of fragments containing GC, G*C and GA, G*A, respectively. It is evident that the parameter α exhibits a marked dependence on the temperature so that in the range 0–40 °C the value of the four samples decreases 2- to 3-fold.

In the model of Allison and Schurr (1979) that we adopted for the derivation of the hydrodynamic parameter of DNA by FPA data, this molecule is assumed to be a string of disks (the base pairs) connected by Hookean springs which can twist and bend. In our samples, owing to the short length, bending is negligible so we are mainly measuring the temperature dependence of torsional deformations along the double helix axis. Recently, the temperature dependence of α was studied by Delrow et al. (1998) on longer DNA fragments of length between 1.7 and 7kbases in the temperature range from 0 to 60 °C. The decrease of α with rising temperature observed by these authors, slightly lower than that we observed, was correlated to secondary structure variations also shown in their samples in CD premelting transitions. Owing to the different length, direct comparison with our results cannot be performed. On the other hand, in our samples we did not observe premelting transitions in CD spectra between 0 and 40 °C (data not shown), as expected for DNA sequences which do not contain dA runs (Chan et al. 1990). The temperature effect on the torsional constant of our samples is possibly due to base stacking variations.

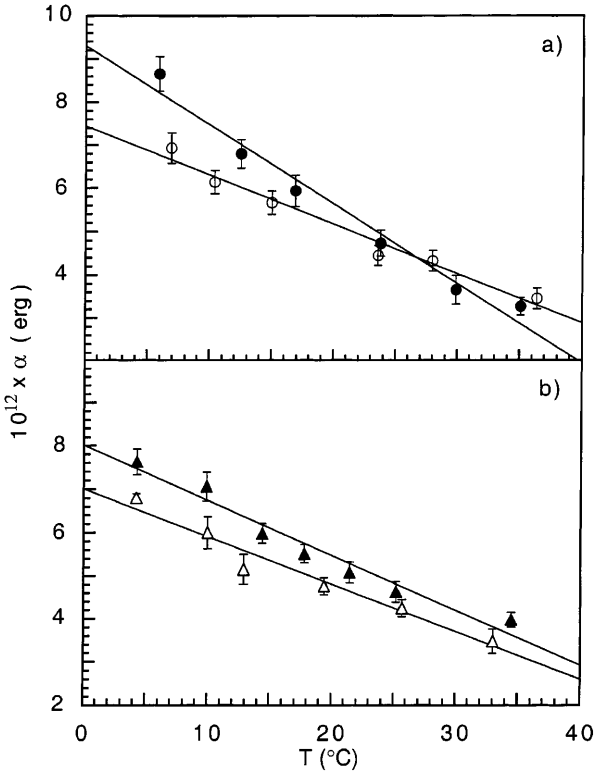

Fig. 5a,b Torsional constant values as deduced by FPA measurements versus temperature for the samples: **a** GC (○) and G*C (●), **b** GA (△) and G*A (▲). Ethidium bromide, at a final concentration of 10^{-6} M, was in a ratio of 1 mole per 200 base pairs of DNA

As already observed in footprinting experiments, GC and GA samples show a very similar behavior in FPA measurements too. Figure 5a, b shows that the slope of the linear fits and the α values are coincident within the error.

The damage introduction in both samples produces an increases of rigidity. This increase is constant in the studied range of temperature for G*A, while it is greater at low temperature for G*C. As a first approximation, we have fitted the data by a linear regression in order to extrapolate the α value at 0 °C, the temperature about which γ-ray footprinting has been performed. The α values are reported in Table 2.

The measured differences of α for the pair of samples G*C-GC and G*A-GA are 1.9×10^{-12} erg and 0.9×10^{-12} erg, respectively. These differences reflect the average increased rigidity experienced by two successive base pairs which oppose the rotational motion of the molecules. The rms average fluctuation of the torsion angle $\langle \Delta\xi \rangle$ between adjacent base pairs in DNA can be obtained by the relation (Barkley and Zimm 1979):

$$\langle \Delta\xi \rangle = \sqrt{\frac{k_B T}{\alpha}} \qquad (2)$$

where k_B is the Boltzmann constant and T the absolute temperature. We calculate a $\langle \Delta\xi \rangle$ value of 4° and 3.6° for GC and G*C, respectively. The average fluctuation of the torsion angle is decreased by 0.4° so that the twist fluctuation of the G*C base pair should be reduced by 12° if all the other base pairs would keep the same rigidity. Footprinting data nevertheless indicate conformational changes up to about 8 bases near the damage, so it can be assumed that the fluctuation decrease is distributed over this range, with an average contribution of about 1.5° per base pair. The same calculation for GA and G*A yields a corresponding value of about 1°, if we consider conformational changes extending up about 10 base pairs in the G*A duplex.

Table 2 Torsional constant values of the control and of 8-oxodG damaged and/or mismatched samples at 0 °C

Sample	α (10^{-12} erg)
GC	7.4 ± 0.2
G*C	9.3 ± 0.2
GA	7.1 ± 0.2
G*A	8.0 ± 0.2

Conclusions

Neither the oxidative damage at G15 nor GA mismatch involve gross alterations of overall structure in the 30-mer fragment studied in this work, as can be observed by conventional spectroscopic analysis. Weak destabilization is exhibited only by the mismatched GA sample.

Finer footprinting analysis shows instead that the presence of 8-oxodG subtly modifies the B DNA geometry of the duplex. An interesting result is that these changes are not localized at the modified base pair but they are extended in a neighboring region of 8–10 base pairs, involving almost one helical turn. G*C and G*A samples share, as a common feature, a reduction of the cutting frequency in a range of 7–8 bases on the 5′-side, indicative of minor groove narrowing.

Some differences are observed in the pattern of the two damaged samples. NMR studies (Kouchakdjian et al. 1991; Oda et al. 1991) have shown that the G*C base pair is in *anti-anti* conformation as GC, with three Watson-Crick H-bonds, while G*A can assume *syn-anti* conformation with two Hoogsteen H-bonds. These different forms have been suggested to be the basis for differential recognizing of G* in Mut M and Mut Y pathway repairs (Grollman and Moriya 1993; Plum et al. 1995). The *syn-anti* conformation of G*A has nevertheless been observed in a sequence context different from that of our fragment, so that we cannot relate different conformations of the glycosidic bond in G*C and G*A to differences observed in footprinting patterns.

On the other hand, the two different conformations of *anti-anti* in GC and *anti-syn* in GA, observed in the same sequence context of our samples (Brown et al. 1986), give a very similar cutting pattern in our footprinting experiments, according to the little modifications of overall and local structure observed with X-ray diffraction methods. This similarity has been considered to be the reason why a considerable fraction of GA mismatches escapes detection by proofreading (Fersht et al. 1982).

The 8-oxodG damage does not change the value of the hydration radius (constant in all the range of temperature analysed also in GA sample), but produces an increase of torsional rigidity in both the duplexes G*C and G*A. The reduction of the average torsional fluctuation of the involved base pairs in the damaged samples ranges roughly between 1° and 2°, indicating that slight effects can also be revealed by the techniques employed.

Acknowledgements This work was partially supported by CNR. We are grateful to Giuseppe Chirico for providing the software for fluorescence polarization anisotropy data fitting. We wish to thank Paola Di Ciaccio for her help in editing the manuscript.

References

Allison SA, Schurr JM (1979) Torsion dynamics and depolarization of fluorescence of linear macromolecules. I. Theory and application to DNA. Chem Phys 41: 35–39

Barkley MD, Zimm BH (1979) Theory of twisting and bending dynamics of short linear DNAs. Analysis of triplet anisotropy decay of a 209 base pair fragment by brownian simulation. J Chem Phys 70: 2991–3007

Barone F, Belli M, Mazzei F (1994) Influence of DNA conformation on radiation-induced single strand breaks. Radiat Environ Biophys 33: 23–33

Barone F, Chirico G, Matzeu M, Mazzei F, Pedone F (1998) Triple helix oligomer melting measured by fluorescence polarization anisotropy. Eur Biophys J 27: 137–146

Barone F, Matzeu M, Mazzei F, Pedone F (1999) Structural and dynamical properties of two DNA oligomers with the same base composition and different sequence. Biophys Chem 78: 259–269

Bertrand HO, Ha-Duong T, Fermandjian S, Hartmann B (1998) Flexibility of the B-DNA backbone: effects of local and neighbouring sequences on pyrimidine-purine steps. Nucleic Acids Res 26: 1261–1267

Breslauer KJ (1994) Extracting thermodynamic data from equilibrium melting curves for oligonucleotide order-disorder transitions. In: S. Agraval (ed) Methods in molecular biology, vol 26. Humana Press, Totowa, NJ, pp 347–372

Brown T, Hunter WN, Kneale G, Kennard O (1986) Molecular structure of the GA base pair in DNA and its implications for the mechanism of transversion mutations. Proc Natl Acad Sci USA 83: 2402–2406

Brown T, Leonard GA, Booth ED, Chambers J (1989) Crystal structure and stability of a DNA duplex containing A(anti)-G(syn) base-pairs. J Mol Biol 207: 455–457

Cantor CR, Warshaw MM, Shapiro H (1970) Oligonucleotide interaction. III Circular dichroism studies of the conformation of deoxyoligonucleotides. Biopolymers 9: 1059–1077

Chan SS, Breslauer KJ, Hogan ME, Kessler DJ, Austin RH, Ojemann J, Passner JM, Wiles NC (1990) Physical studies of DNA premelting equilibria in duplexes with and without homo dA-dT tracts: correlation with DNA bending. Biochemistry 29: 6161–6171

Collini M, Chirico G, Baldini G, Bianchi ME (1995) Conformation of short DNA fragments by modulated fluorescence polarization anisotropy. Biopolymers 36: 211–225

Cridland NA, Saunders RD (1994) Cellular and molecular effects of UVA and UVB. (NRPB-R269), National Radiological Protection Board, UK

Culp SJ, Cho BP, Kadlubar FF, Evans SE (1989) Structural and conformational analyses of 8-hydroxy-2′-deoxyguanosine. Chem Res Toxicol 2: 416–422

Delrow JJ, Heath PJ, Fujimoto BS, Schurr JM (1998) Effect of temperature on DNA secondary structure in the absence and presence of 0.5 M tetramethylammonium chloride. Biopolymers 45: 503–515

Dizdaroglu M (1985) Formation of an 8-hydroxyguanine moiety in deoxyribonucleic acid on gamma-irradiation in aqueous solution. Biochemistry 24: 4476–4481

Fersht AR, Knill-Jones JW, Tsui WC (1982) Kinetic basis of spontaneous mutation. Misinsertion frequencies, proofreading specificities, and cost of proofreading by DNA polymerases of *Escherichia coli*. J Mol Biol 156: 37–51

Franchet-Beuzit J, Spotheim-Maurizot M, Sabattier B, Blazy Baudras B, Charlier M (1993) Radiolytic footprinting. Beta rays, gamma photons, and fast neutrons probe DNA-protein interactions. Biochemistry 32: 2104–2110

Gao X, Patel DJ (1988) G(syn)-A(anti) mismatch formation in DNA dodecamers at acidic pH: pH-dependent conformational transition of G-A mispairs detected by proton NMR. J Am Chem Soc 110: 5178–5182

Grollman AP, Moriya M (1993) Mutagenesis by 8-oxoguanine: an enemy within. Trends Genet 9: 246–249

Grollman AP, Johnson F, Tchou J, Eisenberg M (1994) Recognition and repair of 8-oxoguanine and formamidopyrimidine lesions in DNA. Ann NY Acad Sci 726: 208–214

Kasai H, Crain PF, Kuchino Y, Nishimura S, Ootsuyama A, Tanooka H (1986) Formation of 8-hydroxyguanine moiety in

cellular DNA by agents producing oxygen radicals and evidence for its repair. Carcinogenesis 7: 1849–1851

Kouchakdjian M, Bodepudi V, Shibutani S, Eisenberg M, Johnson F, Grollman AP, Patel DJ (1991) NMR structural studies of the ionizing radiation adduct 7-hydro-8-oxodeoxyguanosine (8-oxo-7H-dG) opposite deoxyadenosine in a DNA duplex. 8-oxo-7H-dG(syn)-dA(anti) alignment at lesion site. Biochemistry 30: 1403–1412

Lin TS, Cheng JC, Ishiguro K, Sartorelli AC (1985) 8-Substituted guanosine and 2'-deoxyguanosine derivatives as potential inducers of the differentiation of friend erythroleukemia cells. J Med Chem 28: 1194–1198

Madge D, Zappala M, Knox WH, Nordlund TM (1983) Picosecond fluorescence anisotropy decay in the ethidium/DNA complexes. J Phys Chem 87: 3286–3288

McAuley-Hetch KE, Leonard GA, Gibson NJ, Thomson JB, Watson WP, Hunter WN, Brown T (1994) Crystal structure of a DNA duplex containing 8-hydroxydeoxyguanine-adenine base pair. Biochemistry 33: 10 266–10 270

Negri R, Costanzo G, Di Mauro E (1991) A single reaction method for DNA sequence determination. Anal Biochem 197: 389–395

Oda Y, Uesugi S, Ikehara M, Nishimura S, Kawase Y, Ishikawa Y, Inoue H, Ohtsuka E (1991) NMR studies of a DNA containing 8-hydroxydeoxyguanosine. Nucleic Acids Res 19: 1407–1412

Packer MJ, Hunter CA (1998) Sequence-dependent DNA structure: the role of the sugar-phosphate backbone. J Mol Biol 280: 407–420

Plum GE, Grollman AP, Johnson F, Breslauer KJ (1995) Influence of the oxidatively damaged adduct 8-deoxyguanosine on the conformation, energetics and thermodynamic stability of a DNA duplex. Biochemistry 34: 16 148—16 160

Sambrook J, Fritsch EF, Maniatis T (1989) Molecular cloning. A Laboratory manual. Spring Harbor Laboratory Press, Cold Spring Harbor, NY

Schurr JM (1984) Rotational diffusion of deformable macromolecules with mean local cylindrical symmetry. Chem Phys 84: 71–76

Sy D, Savoye C, Begusova M, Michalik V, Charlier M, Spotheim-Maurizot M (1997) Sequence dependent variations of DNA structure modulate radiation-induced strand breakage. Int J Radiat Biol 72: 147–155

Ti GS, Gaffney BL, Jones RA (1982) Transient protection: efficient one-flask syntheses of protected deoxynucleosides. J Am Chem Soc 104: 1316–1319

Tirado MM, Garcia de la Torre J (1980) Rotational dynamics of rigid, symmetric top macromolecules. Application to circular cylinders. J Chem Phys 73: 1986–1993

Von Sonntag C (1987) The chemical basis of radiation biology. Taylor and Francis, London

Wang D, Kreutzer DA, Essigman JM (1998) Mutagenicity and repair of oxidative DNA damage: insights from studies using defined lesions. Mutat Res 400: 99–115

Zhang X, Rosenstein BS, Wang Y, Lebwohl M, Mitchell DM, Wei H (1997) Induction of 8-oxo-7,8-dihydro-2′-deoxyguanosine by ultraviolet radiation in calf thymus DNA and HeLa cells. Photochem Photobiol 65: 119–124